12

B.S.

(6) FEASIBILITY OF SPECIAL PURPOSE ATOMIC STANDARD

(11) 1976

(10) David J. Wineland

(12) 34 p.

Sponsored by:

Advanced Research Project Agency

(15) ARPA Order-3140

240800

FINAL REPORT

ARPA Order no.: 3140

Program Code no.: 6G10

Name of Contractor: National Bureau of Standards

Effective date of Contract: December 15, 1975

Contract expiration date: April 30, 1977

Amount of Contract: $100 K

Contract no.: NBS Cost Center 2774441

Program element code: 62702E

Principle investigator: David J. Wineland
(303) 499-1000, ext. 3224

Project scientists: Helmut Hellwig
(303) 499-1000, ext. 3277

David A. Howe
(303) 499-1000, ext. 3209

David J. Wineland
(303) 499-1000, ext. 3224

TITLE: FEASIBILITY OF SPECIAL PURPOSE ATOMIC STANDARD

TABLE OF CONTENTS

		page
	SUMMARY	1
I.	INTRODUCTION	2
II.	$\sim$ 0.5 GHz PRIMARY OSCILLATOR AND DIVIDER	2
III.	STEP RECOVERY DIODE MULTIPLIER	5
IV.	AMMONIA GAS ABSORPTION CELL	5
	(a) Choice of 3-3 Transition in $N^{15}H_3$	6
	(b) Ammonia containment	6
	(c) Microwave cavity for ammonia	7
V.	SERVO SYSTEM	9
	(a) Cavity Pulling	9
	(b) Distortions in the microwave source and detector	11
	(c) Servo phase comparators and integrators	13
VI.	RESULTS	14
	(a) Stability	14
	(b) Accuracy	15
	(c) Systematic frequency offsets	15
	(d) Ammonia containment	17
	(e) Integrator-demodulator stability	17
	(f) Environmental sensitivity	17
VII.	FUTURE PROJECTIONS	19
VIII.	SUMMARY	20
	ACKNOWLEDGEMENTS	20
	REFERENCES	21
	FIGURE CAPTIONS	23

SUMMARY

A special-purpose frequency standard and clock has been developed, featuring a novel combination of stability and accuracy performance, shock and temperature insensitivity, instant turn-on characteristics, and the potential for low weight, power consumption, and low fabrication costs. This device should be able to fill a metrology need not satisfied by presently available atomic and quartz-crystal standards.

The device is based on the well-known 3-3 transition in ammonia ($\sim$23 GHz), which provides the frequency reference for a $\sim$0.5 GHz oscillator. This oscillator is a novel stripline transistor oscillator of high spectral purity. Its output is multiplied in one step to K-band and the resulting output is passed through a waveguide cell containing ammonia. The detected absorption feature is used to frequency lock the 0.5 GHz oscillator to line center. To accomplish this, the oscillator is frequency modulated at $\sim$10 kHz and is locked by nulling the third harmonic of the detected output. This technique discriminates to a high degree the effects of "background slope" pulling. In addition, pulling from the microwave cavity absorption cell is diminished by locking the cavity to the ammonia transition by nulling the fifth harmonic of the detected output. A fixed output frequency between 5 and 10 MHz is provided by direct division from 0.5 GHz.

about

The observed stability is 2×10^{-10} from 10 to 6000 sec., and reproducibility is estimated to be $\pm\ 2 \times 10^{-9}$. The rather broad linewidth of ammonia ($\sim$100 kHz due to Doppler broadening) reduces overall resolution but allows a short ($\gtrsim$0.15 μs) servo attack time, thus reducing the acceleration sensitivity of the primary 0.5 GHz oscillator. In this respect the ammonia absorption device may have a unique advantage. Linewidths of most other precision oscillators are considerably narrower, resulting in longer attack times needed to lock the primary (vibration sensitive) oscillator to the (vibration insensitive) frequency reference. Vibration sensitivities as small as 10^{-11} s^2/m ($10^{-10}/g$) appear feasible. Servo offset problems have been substantially reduced by using digital demodulators in the feedback networks. Working at pressures where collision broadening contributes to the linewidth allows one to easily null out pressure shifts; shifts smaller than 3.8×10^{-9}/Pa ($5 \times 10^{-10}/\mu m$) have been observed. Power consumption should be $<$ 3 W and expected size of a working device $\sim 10^3$ cm^3. With further development, improvements in performance can be expected.

I. INTRODUCTION

The special-purpose ammonia frequency standard has been developed because of the need for an oscillator satisfying specific requirements not found in other precision oscillators. The design and goals of the present project have been discussed elsewhere [1]; briefly we seek an oscillator with accuracy (i.e., long-term reproducibility) in the 10^{-9} range and stability in the 10^{-10} range. Other desirable features to be included are environmental insensitivity, (i.e., low sensitivity to acceleration, temperature, magnetic and electric fields) and instant turn-on capability. Finally it is desirable that the device have low weight and volume and small fabrication cost.

To realize such an oscillator we have investigated the scheme shown in Fig. 1. This basic scheme was used in the first "atomic" clock [2] and was revived because of its simplicity. In Fig. 1 a primary oscillator is referenced to the 3-3 transition in $N^{15}H_3$ (22.79 GHz). For simplicity the frequency of the primary oscillator is chosen to be $\sim$0.5 GHz; this allows one to multiply in one step to the ammonia frequency and at the same time directly divide the oscillator output frequency to produce an output frequency near 5 MHz which is harmonically related to the ammonia frequency. (Multiplication factor = 4400). The oscillator is a simple stripline oscillator, the multiplier uses a waveguide mounted step recovery diode, the ammonia storage vessel is a simple closed cell and the dividers are readily available I. C. modules.

Below we discuss the system and the results obtained. It is convenient to first cover the main components of the system individually: oscillator and divider, multiplier, ammonia cell and microwave cavity, and servo system. We then discuss results obtained on stability, accuracy (reproducibility), ammonia cell development and sensitivity to environmental parameters. Finally, we note future possibilities based on our present results.

II. $\sim$ 0.5 GHz PRIMARY OSCILLATOR AND DIVIDER

In reviewing the possible oscillator designs, it appeared that an oscillator using a simple LC resonator should be investigated. Advantages to this design include:

(1) wide tunability,

(2) continuous operation under very adverse conditions (shock, vibration),

(3) good short-term stability,

(4) low cost.

An oscillator was developed operating at about 0.5 GHz and having a free-running stability as shown in Fig. 2. The curves were obtained with a divider chain ($\div 100$) after the 0.5 GHz oscillator. These data were computed using the two-sample variance for different averaging times [3]. The bandwidth of the measurement system affects the variance in the case of white and flicker of phase type noise; therefore, two curves are plotted around the averaging times of interest ($\sim$10 ms). The oscillator features a P. C. board etched strip as a transmission line resonator (stripline resonator). In the design of a high-performance stripline oscillator, we must address three principal problems [4]:

(1) minimization of resonator losses,

(2) minimization of additive transistor noise, and

(3) shock and vibration isolation of the resonator.

There are other problems which must be looked at, but these three represent the major contributors to degradation in stability.

Radiative loss is minimized by adopting a three-layer sandwich etch technique. In this design, two ground planes are used on the top and bottom surfaces of the P. C. board with the stripline centered in the dielectric. To keep loss to a minimum, fiberglass-teflon which has a small loss tangent of about 10^{-3} is used for the dielectric. The stripline itself is a 7 cm length of copper which is 1 cm wide and 2 mm thick. Contact resistance is minimized by using silver-solder on all connections. The unloaded Q of the resonator at 0.5 GHz is about 400. Loaded Q of the resonator is maximized by the use of a field-effect transistor as the active element [5]. It is chosen to have a high forward transconductance and a high cut-off frequency.

Oscillator noise is generally characterized by low frequency (near carrier) flicker noise behavior and high frequency (far from carrier) white phase noise. Sources of noise may be multiplicative or additive. Causes of flicker behavior are difficult to identify in many instances, but helpful in the reduction of flicker noise is the selection of a transistor which is manufactured with care and in a clean environment, since flicker noise may relate to sporadic conductance through the device due to impurities. White

phase noise is usually associated with additive thermal noise of components and/or transitor parameters. One can resort to devices capable of higher signal levels in order to get above a fixed noise level. A trade-off exists between white phase and flicker noise, however, since higher device currents usually aggravate the flicker noise problem. We have arrived at a compromise solution which gives suitable performance in the NH_3 standard. The curves shown in Fig. 1 represent a higher device drive level than is common in, say, quartz-crystal oscillators.

At frequencies around 0.5 GHz, transistor package parameters (inductance and capacitance) and stray parasitic elements such as connecting lead inductance and stray capacitance all contribute to the fundamental resonance. If one is to achieve a relative frequency stability approaching 1×10^{-9}, then it is imperative to maintain resonator inductance and capacitance values stable to this level. The greatest deterrent to maintaining high inductive and capacitive stability is vibration sensitivity of the oscillator. This problem of microphonics has been reduced by using the three-layer P. C. board and rigidly mounting all components and leads with a low-loss doping compound. The oscillator is in turn rigidly fixed to an aluminum block which acts as the shield for the components. The test block weighs about 3 kg. Depending on the application, one can rigidly mount or soft mount the oscillator into a system. If rigidly mounted, structure-born vibration is directly applied to the oscillator. A soft mount designed to isolate the oscillator from vibration can reduce the transmitted vibration at higher frequencies at the cost of increasing the vibration sensitivity at a lower frequency. Damping material can also be used to alter the vibration response.

In the ammonia standard, the problem of vibration sensitivity of the fundamental oscillator is significant in cases of shock and vibration where the dynamic range of the servo system is exceeded or the period of the vibration is shorter than the servo attack time. A key incentive for choosing a wide spectral line is that the servo attack time can be small. Since the NH_3 resonance is ~100 kHz, this enables the use of fast loop response. The design of the oscillator mount should yield a vibration response in which frequencies of ~100 kHz and above are suitably attenuated.

The division from 500 MHz to 5 MHz uses one ECL decade divider followed by a TTL decade divider (from 50 MHz to 5 MHz). A level translator was used

between these I.C.'s. The ECL divider contained an internal wideband amplifier thus allowing good isolation between divider logic and the source. In short term (<10 ms), the white phase noise of the dividers set a limit on the stability at 5 MHz.

III. STEP RECOVERY DIODE MULTIPLIER

It is desirable to make a multiplier module with fairly low output Q ($Q \lesssim 10$) and output power $\gtrsim 10\ \mu W$. We use state-of-the-art step-recovery diodes in a waveguide multiplier module (See Fig. 3.). In simplest terms, the problem is one of impedance matching for both the input and output circuit. For example, for the input circuit (~ 0.5 GHz) the dynamic diode impedance is $Z \simeq 1\Omega$. Therefore, two π section transformers are cascaded to match to the 50Ω output impedance of the 0.5 GHz amplifier. Approximately 0.5 W input power is needed to "snap" the diode properly. To accomplish this, a microstrip hybrid class "C" amplifier is used. The amplifier, microstrip matching circuit and multiplier module are integrated into one package in order to avoid instabilities due to connections. The output circuit is composed of a shorting stub and iris coupling to form a cavity ($Q \simeq 10$) with the diode approximately matched to the characteristic impedance of the narrow height waveguide. In the interest of rigidity and simplicity, shims are used rather than movable plungers. With ~ 0.6 W input power to the diode, output power of approximately 100 μW was obtained.

IV. AMMONIA GAS ABSORPTION CELL

The advantages of using ammonia as the reference "atom" are:

(1) The microwave transition of interest provides an absorption signal which is orders of magnitude stronger than those of other interesting molecules or atoms [6]. This is a significant advantage because it means that the desired signal-to-noise is obtained without resorting to impractically large microwave cell sizes as would be necessary for almost any other gas cell.

(2) Since ammonia remains in the gas phase for the temperature range of interest (-40° to +60°C) the device has instant turn-on capability. One must, however, note the existence of a pressure (therefore temperature) dependent frequency shift; this is discussed more fully below.

(3) The frequency of the ammonia transition is fundamental in nature and therefore essentially eliminates the need for calibration of the device.

(4) The ammonia transition linewidth is fairly broad ($\sim$100 kHz). This is a disadvantage in terms of the ultimate accuracy obtainable, but it allows the primary oscillator to be locked to the ammonia reference in very short times ($\gtrsim$1.5 μs). This allows a significant reduction in the acceleration sensitivity of the primary oscillator.

(a) Choice of 3-3 Transition in $N^{15}H_3$

The reference transition was chosen to be the 3-3 line in ammonia because of its large signal strength [6]. The $N^{15}H_3$ isotope was chosen because the N^{15} nucleus has no quadrupole moment and therefore it is free of the quadrupole structure which makes the 3-3 line of the $N^{14}H_3$ isotope asymetric. This asymmetry causes the apparent line center to depend on FM modulation amplitude and microwave power. Uncertainties as large as approximately 4 x 10^{-8} could be expected from this asymmetry.

The results of three high resolution determinations of the 3-3, $N^{15}H_3$ frequency are:

$$\nu_o = 22\ 789\ 421\ 731 \pm 1 \text{ Hz} \quad [7]$$

$$\nu_o = 22\ 789\ 421\ 701 \pm 1 \text{ Hz} \quad [8]$$

$$\nu_o = 22\ 789\ 421\ 672 \pm 55 \text{ Hz} \quad [9].$$

These measurements were taken with ammonia beam masers and show that although rather high resolution can be obtained, a conservative uncertainty in one's knowledge of the frequency is about 10^{-9}, For our work we therefore assume:

$$\nu_o = 22\ 789\ 421\ 700\ (1 \pm 10^{-9}) \text{ Hz}.$$

(b) Ammonia Containment

Most aspects of the present device could be tested in an experimental apparatus using a gas flow system for the ammonia [1]. A simple gas flow system could be used in the final device but the added complexity is a disadvantage. Therefore, it is desirable to develop permanent closed cells.

The problem of ammonia containment is well known; in a simple cell using brass or copper waveguides, reaction of ammonia with the cell walls causes rapid disappearance of the signal particularly if water vapor is present or the waveguide walls are not sufficiently clean. Also, even in a clean environment, chemisorption with certain metals is noted [10]. Various inert cell coatings were considered [1], however it was felt that a simpler approach would be to make cells from inert materials whose cleanliness could be insured.

Two basic problems are encountered in obtaining such a cell: (1) a provision must be made for evacuating, baking, and cleanly sealing the cell, (2) the cell must form part of or be included in a microwave cavity for interrogation by the microwave radiation. This implies that the material used for the windows must be nearly lossless and be easily bonded to the rest of the cavity. Two basic schemes were tried and although not enough work has been completed on cell development, the results are encouraging.

First cells were made with quartz cylinders of rectangular cross section which could be inserted into X-band waveguide. Both ends were extended and drawn into points to provide a seal. Quartz was used because its microwave losses are negligible. The cells were baked under vacuum at 300°C for 30 hours at a pressure of $< 10^{-4}$ Pa (1 Torr $\simeq$ 133 Pa). Ammonia was then backfilled at pressures between 0.13 and 0.67 Pa (10^{-3} Torr to 5×10^{-3} Torr). No attempt was made to purify the ammonia which was contained in a lecture bottle and admitted to the cell through a metal leak valve. The cells were then sealed off by heating a quartz pinch-off.

A second type of cell was made of stainless steel K-band waveguide. Windows were made of quartz which were mated to brass flanges with pressed indium seals. Ammonia was admitted through a copper pinch-off which was silver soldered to the broad face of the waveguide in which small holes were drilled. The cells were baked at 100°C for 50 hours at a pressure of $< 10^{-4}$ Pa. The gas was admitted as above (without purification) and the copper pinch-off was then sealed.

(c) Microwave Cavity for Ammonia

Conceptually, the simplest approach would be to pass the microwaves through the ammonia and servo the frequency of the oscillator to the point of

maximum absorption. No errors would occur with this method if there were no reflections at the ammonia cell interface and if the source and detector were perfectly matched to the microwave guide. Such is hardly the case in practice and since reflections occur at both sides of the ammonia cell, it is effectively contained in a cavity.

Frequency pulling due to cavity mistuning is a familiar problem to designers of atomic clocks. In a passive standard such as the one discussed here, the frequency ν at which microwave absorption is maximum is given by [11]:

$$(\nu - \nu_o) = \frac{Q_c}{Q_\ell} (\nu_c - \nu_o) \tag{1}$$

where ν_o = unperturbed ammonia frequency

ν_c = cavity center frequency

Q_c = microwave cavity Q

Q_ℓ = ammonia transition Q

and the expression is valid when: $(\nu_c - \nu_o)/\nu_o << 1/Q_c$, $Q_\ell >> Q_c$.

This result follows simply from the fact that the ammonia and microwave cavity form a system of coupled oscillators. Therefore varying the frequency of the cavity changes the apparent frequency of the ammonia line. In a cavity formed from a section of waveguide the importance of reflections is illustrated by example: If we made an ammonia cell from a section of copper WR-42 waveguide of length ℓ and if the windows had (real) voltage reflection coefficients of value Γ_v, then the effective Q of the resulting cavity is given by:

$$Q_c = 4\pi\ell \ \lambda_g \Gamma_v / \lambda_o^2 \tag{2}$$

where λ_g = guide wavelength

λ_o = free space wavelength.

If we choose $\Gamma_v = 0.2$, $\ell \simeq 50$ cm [12] and since $\lambda_g \simeq 1.59$ cm, $\lambda_o = 1.31$ cm at the frequency of interest then $Q_c \simeq 115$. From Eq. 1, we see that we would have to tune the cavity to 0.02% of its linewidth to obtain 10^{-9} accuracy in the output frequency. Since the expansion coefficient for copper is $\alpha_c = 1.5$

$\times 10^{-5}$/°C and $Q_\ell \approx 2 \times 10^5$ then the frequency dependence on temperature due to cavity pulling would be:

$$\frac{\partial \nu}{\partial T} = \frac{Q_c}{Q_\ell} \alpha \approx 10^{-8}/°C.$$

Because of this rather strong sensitivity and because it is difficult to make reflectionless windows for the cavity, one must servo the cavity to line center. A few possibilities exist for accomplishing this. One is to separately sense the cavity frequency with microwave power applied symmetrically to either side of the cavity resonance [13]. However, frequency-to-amplitude conversion is a severe problem with the low cavity Q obtained here and such a method is precluded. If Q_ℓ could be varied, then one could look for zero change in output frequency when this is done; this assures $\nu_c - \nu_o = 0$ in Eq. 1. This could be accomplished by symmetrically broadening the line by applying a magnetic field [14]. Unfortunately this broadening is only $\sim$ 7 MHz/T (1 G ss = 10^{-4}T) and therefore a rather large magnetic field modulation is required to appreciably broaden the line. Another disadvantage of this scheme is that it requires a second reference oscillator in order to detect frequency changes when the magnetic field is changed.

A third method exists and, to the authors' knowledge, has not been used previously. It is discussed in the next section.

V. SERVO SYSTEM

The basic requirement of the servo system is that it force the frequency of the primary oscillator ($\sim$ 0.5 GHz) to be at a subharmonic of the ammonia transition frequency. Of course, various systematic effects shift the apparent frequency of the ammonia transition; these must either be eliminated or controlled in a known way. Although the performance of the device is not high when compared to a state-of-the-art atomic clock, the demands on the servo system are rather high. This is because we are trying to resolve the rather broad resonance feature (i.e., "split the line") to about 10^{-5} or 0.001 percent. Therefore, state-of-the-art techniques must be employed. Below we discuss the effects of cavity pulling, distortions in the source and detector and servo offsets and drifts.

(a) Cavity Pulling

We assume here that the microwave source and detector are perfectly flat, that is, the power output from the source and the detected power do not depend on frequency. Eq. 1 yields the frequency ν where the absorption is a maximum.

To facilitate the detection of this condition, source frequency modulation is used. This technique is well known and is used in other atomic clocks including cesium, rubidium, and the passive hydrogen standard [15]. Basically, we frequency modulate the source at frequency ν_m so that the time dependence of the microwave field from the source is:

$$E = E_o \cos\left(\omega_s t + \frac{\Delta\omega}{\omega_m}\cos\omega_m t + \phi\right),$$

where ω_s = average frequency of source,

$\Delta\omega$ = peak frequency excursion,

ω_m = $2\pi\nu_m$ (angular modulation frequency),

ϕ = arbitrary phase angle,

$\Delta\omega/\omega_m$ modulation index.

When $\nu_s - \nu_o \lesssim \Delta\nu_\ell$ ($\Delta\nu_\ell$ = ammonia linewidth) the detected signal will have an oscillating component at frequency ν_m; the phase and amplitude of this component will vary as a function of frequency as shown in Fig. 4(a). These curves are the voltages observed at the outputs of the mixers in Fig. 5. This "dispersion" curve is used to servo the primary oscillator to the apparent line center by finding the condition at which the dispersion curve has zero output. When $\Delta\omega/\omega_m << 1$, the frequency at which this occurs is given by Eq. 1. However, for $\Delta\omega/\omega_m \approx 1$, Eq. 1 must be slightly modified. Also we note the appearance of higher harmonics of ν_m in the detected output; in particular, the amplitudes and phases of the higher odd harmonics have similar "dispersion" characteristics. Figures 4 (b) and (c) show the dispersion curves for the third and fifth harmonics respectively when $\Delta\omega/\omega_m$ is adjusted to give maximum slope near the center of the pattern. (Vertical scales are changed for each part of Fig. 4.) We can then use the dispersion curves of the higher harmonics to lock to line center. Two important points should be made:

(1) For large modulation amplitudes $\Delta\omega/\omega_m \gtrsim 1$ it can be shown that Eq. 1 is modified to the form:

$$\nu - \nu_o = K(n) \frac{Q_c}{Q_\ell}(\nu_c - \nu_o) \qquad (3)$$

where K(n) is close to unity but varies by factors of two or three as $\Delta\omega$ is varied. It is also a function of the harmonic number observed (n) and in

general $K(n) \neq K(n')$ for the same $\Delta\omega$. We have used this last fact to simultaneously servo the oscillator and cavity to line center therefore avoiding cavity pulling. As shown in Fig. 5, the third harmonic dispersion is used to lock the multiplied primary oscillator to apparent line center, i.e., the condition:

$$\nu - \nu_o = K(3) \frac{Q_c}{Q_\ell} (\nu_c - \nu_o) \qquad (4)$$

is satisfied. The fifth harmonic dispersion is used to lock the cavity to the line center, i.e., the condition:

$$\nu - \nu_o = K(5) \frac{Q_c}{Q_\ell} (\nu_c - \nu_o) \qquad (5)$$

is satisfied. Since $K(3) \neq K(5)$, conditions (4) and (5) can be satisfied simultaneously only if $\nu_c - \nu_o = \nu - \nu_o = 0$.

(2) The use of the above scheme causes some loss of signal strength; to give an idea of this loss we have measured the ratio of the slopes [SL(n)] of the dispersion curves when the microwave power is kept fixed and when the slope is maximized for each harmonic.

We measured:

$$SL(1) : SL(3) : SL(5) = 1.0 : 0.42 : 0.26$$

From the standpoint of signal strength it would be better to use the fundamental and third harmonic locks in the above scheme;however, conditions (outlined later) led us to choose the third and fifth harmonic locks. We note that a further slight reduction in signal strength or slope ($\gtrsim 10\%$) is observed when the system is optimized for the third and fifth harmonic locks simultaneously.

The microwave cavity is formed by a combination of shunt impedances due to the windows and added reactances at both ends of the ammonia cell. Electronic tuning is provided by a varactor diode at one end of the cell.

<u>(b) Distortions in the microwave source and detector</u>

In general, the source and detector are not "flat" with frequency; that is, frequency to amplitude conversion occurs which shifts the apparent frequency of the ammonia transition. The most serious problem occurs in the

source. Briefly, frequency-to-amplitude conversion occurs because of the (slightly mistuned) reactances in the source. In time domain, a qualitative picture is given by assuming that as the frequency of the source swings below ν_o, its amplitude increases; as its frequency swings above ν_o, its amplitude decreases. Assuming that $\nu_c = \nu_o$, and $\nu_s = \nu_o$, then the signal from the ammonia absorption would be stronger on the low side of ν_o than on the high side. Equivalently, there exists a residual signal component at ν_m (and $3\nu_m$ and $5\nu_m$) on the detector which the servo then compensates for by shifting ν_s to a value below ν_o. Since $\Delta\omega/2\pi \simeq \Delta\nu_\ell$ in practice, then if AM of amplitude β exists as discussed above, we would have:

$$(\nu_s - \nu_o) \simeq -\beta\Delta\nu_\ell \tag{6}$$

in the locked condition. This pulling is accentuated for the fundamental dispersion lock (at ν_m) if the signal from the ammonia is only a small fraction (γ) of the signal reaching the detector because essentially all of the AM on the input rf reaches the detector even in the absence of ammonia. In this case:

$$(\nu_s - \nu_o) \simeq -\frac{\beta}{\gamma}(\Delta\nu_\ell) \text{ (fundamental lock).}$$

However, for the third and fifth harmonic locks, Eq. 6 applies to a high degree the third and fifth harmonics appear at the detector only because of the presence of ammonia. This is one reason for using the higher harmonic locks.

If the source is "flat" with frequency and the detector is not, the problem is not as severe as it is for the source. Since we are locking to the third and fifth harmonics of ν_m then spurious third or fifth harmonic signal is generated only because the curvature (nonlinearity) of the detector converts the FM (at frequency ν_m) into AM at frequency $3\nu_m$ or $5\nu_m$. Since the curvature of the detector should be small this type of offset should be negligible. This is another reason for using the third and fifth harmonic locks as noted in Sect. V(a). Third harmonic lock of the primary oscillator [16] also discriminates against background slopes (for example, due to overlapping transitions) but this is not a problem for the ammonia device.

In general, it is easier to make the detector flat and control its flatness than it is for the source. Therefore, we have servoed out the AM (at frequency ν_m) in the source by nulling the signal (at ν_m) observed at the detector. Since the detector may not be perfectly flat, this introduces a systematic offset of the type in Eq. (6). It is important that this residual slope in the detector remain fixed in order to assure long-term stability and reproducibility. As noted below in Sect. VI(c), it may be desirable to make a detector with a specific slope which can be used to compensate the frequency shift due to pressure.

It is critically important to null the fundamental frequency signal component (ν_m) at the detector for another reason. If this is not done, then signal at ν_m can mix in the detector with the rather strong signals at $2\nu_m$ and $4\nu_m$ to give signals at $3\nu_m$ and $5\nu_m$ which gives further offsets. These offsets are avoided by exactly nulling the fundamental signal component of the detected output.

Finally, one must insure that FM distortion does not occur at the oscillator. For example, second harmonic FM distortion [17] due to a signal component of frequency $2\nu_m$ at the FM input causes a signal component at $3\nu_m$ at the detector because of the strong nonlinearity of the ammonia line. For the ammonia device, such distortion is avoided by insuring that the second harmonic of the FM input is $\gtrsim$ 75 dB down from the fundamental. This is easily accomplished with passive filtering.

(c) Servo phase comparators and integrators

Conventional analog phase comparators have output voltage offsets due to an asymmetry which may exist in the signal switching portion of the device. Here the signal from the microwave detector undergoes a 180° phase reversal at each half-cycle of the reference signal (third or fifth harmonic of modulation frequency). The signal path through the comparator for one half-cycle versus the other half-cycle must be identical to realize zero offset; however, this is difficult to achieve and therefore offsets will exist. These offsets not only affect the accuracy of the locked oscillator but also the stability, since they are observed to change in time.

The phase comparator is followed by an integrator to realize a second-order loop filter. Analog integrators suffer from input voltage offsets. Furthermore, the common analog integrators, having a capacitor in the negative feedback path, have finite DC gain set by the amplifier; a practical limit is about 140 dB. Capacitor leakage also degrades the analog integrator's performance.

A new phase comparator and integrator has been designed and built which employs digital electronics and can directly replace currently used analog circuitry. Since the line-splitting goal in the ammonia standard is high ($\sim 1 \times 10^{-5}$) to achieve 10^{-10} stability and the offset must be $\sim 1 \times 10^{-4}$ or lower, there was incentive to pursue techniques other than analog. Virtues to the digital system are:

1. negligible voltage offset
2. no capacitor, hence no leakage
3. infinite gain at D.C.
4. excellent low pass filter characteristics
5. excellent environmental immunity.

These positive aspects were weighed against the following observed shortcomings:

1. lower useful modulation rates necessary
2. quantization noise (additive white noise).

At modulation frequencies approaching a few kilohertz, the analog comparator and integrator begins to outperform the digital approach with regard to usable feedback gain and additive noise. The ultimate servo for the ammonia device (which can use modulation frequencies approaching 100 kHz) is one using both analog and digital techniques: the analog portion to respond in short-term and digital portion to respond in long-term.

VI. RESULTS

(a) Stability

A plot of the frequency stability obtained with the ammonia based oscillator is shown in Fig. 2. These data were computed using the two sample variance for different averaging times [3]; frequency drift has not been removed. The results using the free running ~ 0.5 GHz stripline

oscillator have been discussed in Sect. II above. The data shown for 10^{-2} sec to 10 sec were taken with the oscillator locked to the apparent line center using third harmonic ($3\,\nu_m$) dispersion lock discussed in Sect. V; the cavity was unlocked for this data. The longer term data (10 sec to 6×10^3 sec) were taken with the complete system shown in Fig. 5 using a cell volume of 230 cm^3 to increase signal strength. In both cases data were taken with a gas flow system in order to directly monitor pressure; the problems of stability and cell-cavity design have been separated to simplify development.

The shorter term data were taken with a small cell (25 cm^3) to illustrate the relatively good stability obtained with small cell sizes. When the short term data (locking only the oscillator) were taken with the larger cell, (230 cm^3) approximately a factor of five improvement in stability was observed between 10^{-2} sec. and 1 sec. The cause of the flicker behavior (flattening of the $\sigma_y(\tau)$ curve) is not understood at this time but improvements could be expected, thus improving the stability by at least a factor of five over the whole range.

(b) Accuracy

For the reasons outlined in Sect. VI(c) below, accuracy obtained will depend on system parameters such as ammonia pressure and detector slope. Since one is really interested in frequency reproducibility between units and over long periods of time (years), the reproducibility and stability of these system parameters is of primary importance. We estimate that the accuracy obtained in the above sense is approximately $\pm 2 \times 10^{-9}$ if the detector slope can be held to $\pm$ 2% of its initally set value. This estimate is explained below; data is still needed in very long term and between different systems.

(c) Systematic frequency offsets

It is felt that the two most important systematic frequency shifts are those due to pressure and detector slope. Assuming the detected fundamental (signal at ν_m) has been electronically nulled, then there can still be a systematic offset if the detector is not flat; this offset is expressed by Eq. (6) where β is the AM of the rf and where we have assumed

that the total rf signal is much larger than that due to the ammonia ($\gamma <<$ 1). [This is the case except when the cell is very long (~10 m) and/or the reflection coefficients at the cell cavity interfaces are very high.] $\Delta\nu_\ell$ is written approximately as [6,14,18]:

$$\Delta\nu_\ell = \left[(\Delta\nu_o)^2 + (\Delta\nu_p)^2\right]^{1/2}$$

where $\Delta\nu_o$ (~ 100 kHz) is the line broadening due to all causes (primarily Doppler effect) except for ammonia-ammonia collisions, and $\Delta\nu_p$ is the linewidth due to collisions (pressure).

The frequency shift due to pressure is written as:

$$\delta\nu_p = \alpha\, \Delta\nu_p$$

where $\alpha \simeq 0.01$ [19]. Therefore, the total shift due to detector slope and pressure is given by:

$$\delta\nu = \beta \left[(\Delta\nu_o)^2 + (\Delta\nu_p)^2\right]^{1/2} + \alpha\, \Delta\nu_p.$$

The important point to note is that at high pressure ($\Delta\nu_p >> \Delta\nu_o$) we have:

$$\frac{\partial\,(\delta\nu)}{\partial\Delta\nu_p} \simeq \beta + \alpha$$

Therefore, if $\beta \cong -\alpha$, then the change in frequency with change in pressure is very small, therefore reducing pressure (and temperature) shifts. For this condition, when $\Delta\nu_p << \Delta\nu_o$ then $\partial(\delta\nu)/\partial\,\Delta\nu_p \simeq \alpha$. Experimental verification of this is given in Fig. 6 where we have plotted fractional frequency offset (from an arbitrary reference point) versus pressure. We note that at high pressure ($P \gtrsim 0.2$ Pa) that a factor of 2 change in pressure gives a fractional change in frequency of less than 10^{-9}.

Therefore, one could hope to set the detector slope such that $\beta \cong -\alpha$ and greatly reduce pressure (and temperature) sensitivity. If β changes, however, then the frequency would change so that at high pressure ($\Delta\nu_p > \Delta\nu_o$):

$$\frac{\partial(\delta\nu/\nu_o)}{\partial\beta/\beta} \simeq \beta \frac{\Delta\nu_p}{\nu_o} .$$

If $\Delta\nu_p \simeq$ 230 kHz, $\beta \cong \alpha = 0.01$, then if β changed by 1%, the output frequency would change by $\sim 10^{-9}$. More work is needed to improve the above scheme and of course other pressure compensation schemes are possible.

(d) Ammonia containment

Work with closed ammonia cells needs further development but first results are encouraging. For both types of cells the pressure appeared to stabilize about two days after sealing the cell. (Observed signal dropped 30% initially.) First results indicate the stainless steel waveguide cells to be slightly better and after initial stabilization signal degradation was less than 10% after a few weeks. Future work is needed to insure cleanliness and integrity of the cells and better results are anticipated (See Sect. VI.f.(2) below).

(e) Integrator-demodulator stability

The analog and digital demodulators can both be set to give initial offsets corresponding to frequency inaccuracies of less than 10^{-10}. Therefore it is critical that their drift be minimal. To check this, the system was first locked using the digital servoes. The input signal was then also applied to the inputs of separate digital and analog demodulators and the outputs were monitored in time. If no drifts exist in these separate demodulators the output should remain constant in time. Fig. 7 shows the results of a typical measurement of this kind. The analog demodulator was the better of two commercially available high performance lock-in amplifiers. Over about a 20 minute period, the digital offset drift was smaller by more than an order of magnitude over the analog offset drift. The vertical scale in Fig. 7 is calibrated in terms of the equivalent fractional frequency offset of the primary oscillator; it therefore appears that the digital system is adequate. Efforts continue however to find better analog demodulators.

(f) Environmental sensitivity

(1) Vibration sensitivity

Because of the fast servo attack time allowed in the ammonia standard, sensitivity to vibration should be low. This is true to the extent that

the apparent absorption line is stable and that there is sufficient servo gain at the vibration frequency.

The effect of vibration suppression can be seen by observing the spectral density of phase fluctuations $S_\phi(f)$ of the 500 MHz oscillator under vibration. An example of such a measurement is shown in Fig. 8; one curve has the oscillator locked to the ammonia and the other with it unlocked. Vibration frequency is 40 Hz sine with a peak acceleration of $5 m/s^2$. We see at least 45 dB reduction of the power in the 40 Hz additive phase spectral component when the oscillator is locked. This represents an acceleration sensitivity of at most 5×10^{-11} s^2/m $(5 \times 10^{-10}/g)$.

In a systems design, it is desirable to build and mount the oscillator so that vibration sensitivity is as low as possible for vibration frequencies outside the servo loop bandwidth. Since the bandwidth can be made wide in the case of the NH_3 standard (approaching 100 kHz), some flexibility exists in the choice of the oscillator's mechanical design and supporting structures (see Sect. II.)

(2) Temperature sensitivity

Temperature will affect the most critical parameters affecting accuracy and long-term stability; i.e., pressure and detector slope (see Sect. VI.c.). Data was not taken on detector slope; however, to obtain $\pm 2 \times 10^{-9}$ accuracy, the slope of the detector must be maintained to about 2% over the operating temperature of the device.

Pressure sensitivity to temperature was estimated by measuring signal strength as a function of temperature on the sealed stainless steel waveguide. In this way we observed a sensitivity of $1/P\ \partial P/\partial T \simeq 0.05/°C$. That is, a change of 5% in pressure was observed for a change in temperature of 1°C. If the compensation scheme of Sect. VI.c is used, this gives a temperature coefficient of $\simeq 5 \times 10^{-11}/°C$. However, for good accuracy and stability at low ambient temperatures, some minimal temperature servoing may be required. For example, one could servo the temperature to always give a fixed signal by observing the 2nd harmonic signal at the detector.

(3) Electric and magnetic field sensitivity

Electric fields are only of importance in the construction details of the gas cell where thermo-electric and contact potential problems may be

present. A worst estimate can be based on the most sensitive hyperfine component of the (3-3) line; for this we have a relative shift of about $10^{-9} E^2$ (E in V/cm). Since electric fields surely can be limited to less than 0.1 V/cm, this does not appear to be a problem.

To first order, application of magnetic fields causes only a broadening of the ammonia line. This broadening has been observed to be [14]:

$$\frac{\partial (\Delta\nu_\ell)}{\partial H} = 7 \times 10^3 \text{ kHz/T} \quad (1\text{T} = 10^4 \text{ Gauss})$$

If the pressure shift compensation scheme of Sect. VIc is used, then a residual frequency shift due to magnetic field will exist:

$$\frac{1}{\nu_o} \frac{\partial(\delta\nu)}{\partial H} \simeq \frac{\partial(\delta\nu)}{\partial(\Delta\nu_\ell)} \frac{\partial(\Delta\nu_\ell)}{\partial H} = 3 \times 10^{-4} \alpha/\text{T}$$

$$= 3 \times 10^{-6}/\text{T} = 3 \times 10^{-10}/\text{G}.$$

Therefore in extreme magnetic field environments some simple magnetic shielding may be required. The second order Zeeman effect is extremely small; the relative shift is about $2 \times 10^{-7} H^2$ (H in Tesla) and is therefore negligible [8].

VII. FUTURE PROJECTIONS

At the present time a fully integrated prototype has not been constructed; for simplicity the separate aspects of the device were investigated individually. However, some estimates of physical parameters can be made based on the present results

(a) Size requirements The lower limit on size will primarily be limited by the size of the ammonia cell. It is expected that the cell should occupy no more than 1 liter volume; hence the overall package may be from 1-2 liters in volume.

(b) Weight requirement With proper choice of materials the expected final package weight should be less than 2 kg. For operation in extreme magnetic fields, shielding may have to be included; this will increase weight by approximately 1/2 kg.

(c) Power requirements The basic electronic components of the present configuration are shown in Fig. 5 .

The power requirements for specific portions at present:

(1)	0.5 GHz oscillator, 0.5 GHz amplifier with multiplier	5.5 W
(2)	divider chain ($\div 100$)	1.0 W
(3)	detector amplifier and servoes	1.0 W
		7.5 W

The 0.5 GHz power amplifier is the major drain on the power supply. Since the multiplier step-recovery diode needs about 3/4 W input, and the efficiency of the amplifier could be $\sim 60\%$, improvements are expected. In an actual system we could expect total power requirements to be less than half of their present value or ~ 3 W.

VIII. SUMMARY

Although the results obtained with the present device are encouraging, one could hope for even better results with future development. For example, the vibration sensitivity of the device was studied only very briefly but initial results show potential for unsurpassed acceleration insensitivity. Similarly, other aspects of the device could be improved with further work.

The largest uncertainty exists in the control of the AM distortion (detector slope) and pressure shift; and efforts should be concentrated in this area. It should be noted that it is possible to use different approaches for these problems. For example, one could modulate the source at two different frequencies and with different amplitude; this would allow one to independently servo the detector slope to zero thus eliminating AM distortion entirely. (Similar to the 3rd and 5th harmonic locks used to servo the oscillator and cavity). One is then left with the raw pressure shift which could be compensated in the output frequency by, for example, applying a calibrated correction voltage at the integrator input based on the observed signal amplitude.

ACKNOWLEDGEMENTS

The authors wish to thank the other members of the Frequency and Time Standards Section of NBS for their help and encouragement. M.B. Mohler carried out most of the electronics construction; H.E. Bell gave much help in the construction of the physical components. We thank F.L. Walls, S.R. Stein, R.M. Garvey. S. Jarvis, Jr., A.S. Risley and T.C. English (Efratom Inc.) for useful ideas and encouragement during the course of the work.

REFERENCES

[1] WINELAND, D.J., HOWE, D.A. and HELLWIG, H., "Special Purpose Atomic (Molecular) Standard," to be published in the Proc. 8th Annual Precise Time and Time Interval (PTTI) Planning Meeting, December 1976.

[2] LYONS, H., Annals New York Adac, Sci., 55, 831 (1952).

[3] ALLAN, D.W., "Statistics of Atomic Frequency Standards," Proc. IEEE, 54, February 1966, pp. 221-230.

[4] HODOWANEC, G., "Microwave Transistor Oscillators," RCA Application Note AN 6291.

[5] OXNER, E., "High Performance FETs in Low Noise Oscillators," Siliconix Incorporated, December 1973.

[6] TOWNES, C.H., SCHAWLOW, A.L., Microwave Spectroscopy, McGraw-Hill Book Co., New York, 1955.

[7] De PRINS, J., MENOUD, C., and KARTASCHOFF, P., "$N^{15}H_3$ Double Beam Maser as a Primary Frequency Standard," Rev. of Sci. Inst. Vol. 32, No. 11, Nov. 1961, pp. 1267-1268.

[8] De PRINS, J., "$N^{15}H_3$ Double Beam Maser as a Primary Frequency Standard," IRE Trans. on Instr., Vol. I-11, Dec. 1962, pp. 200-203.

[9] KUKOLICH, Steven G., "Measurement of Ammonia Hyperfine Structure with a 2-Cavity Maser," Phys. Rev., Vol. 156, No. 1, April 1967, pp. 83-92.

[10] HAYWARD, D.O., and TRAPNELL, B.M.W., Chemisorption, 2nd Edition. Butterworths, Washington, 1964, pp. 205-248.

[11] VIENNET, J., AUDOIN, C. and DESAINTFUSCIEN, M., "Cavity Pulling in Passive Frequency Standards," IEEE Trans. on Instrm. and Meas., Vol. IM-21, No. 3, August 1972, pp. 204-209.

[12] The length of the waveguide between reflection points must be approximately equal to an integral number of half-wavelengths.

[13] WALLS, F.L., "Design and Results from a Prototype Passive Hydrogen Maser Frequency Standard," to be published in the Proc. 8th Annual Precise Time and Time Interval (PTTI) Planning Meeting, December 1976.

[14] SHIMODA, K., "Atomic Clocks and Frequency Standard on Ammonia Line I," and "III" J. Phys. Soc. Japan 9, June 1954, pp. 378-386 and pp. 567-575.

[15] See for example: HELLWIG, H., "Atomic Frequency Standards: A Survey," Proc. IEEE, Vol. 63, No. 2, Feb. 1975, pp. 212-229. AUDOIN, C. and VANIER, J., "Atomic Frequency Standards and Clocks," J. of Phys. E: Sci. Instr. Vol. 9, 1976, pp. 697-720.

[16] WALLARD, A.D., J. Phys. E. 5, 927 (1972).

[17] SHIRLEY, J.M., "Some Causes of resonant frequency shifts in atomic beam machines, II. The effect of slow frequency modulation on the Ramsey line shape," J. Appl. Phys., Vol. 34, pp. 789-791, 1963.

[18] A more exact treatment when both pressure and Doppler effects are important has been given by: PARSONS, R.W., and ROBERTS, J.A., "The Doppler Contribution to Microwave Line Widths," J. of Mole. Spec. 18, 1965, pp. 412-417.

[19] HEWITT, P.L. and PARSONS, R.W., "Collision Broadening and Shifting in the Inversion Spectrum of NH_3," Phys. Lett., Vol. 45A, No. 1, Aug. 1973, pp. 21-22.

FIGURE CAPTIONS

FIG. 1 Simplified block diagram of system. Frequency lock servo is used employing 0.5 - 25 kHz FM on $\sim$ 5 GHz oscillator.

FIG. 2 Frequency stability plots showing the two sample variance (σ_y) for different averaging times (τ). B.W. $\equiv$ measurement system bandwidth.

FIG. 3 Cross-section of step-recovery diode multiplier module.

FIG. 4 Dispersion curves obtained at output demodulator for different harmonics: (a) fundamental, (b) third harmonic, (c) fifth harmonic. Vertical scales are different in the three cases and curve (c) has an (arbitrary) 180° phase shift introduced.

FIG. 5 Detailed block diagram of system.

FIG. 6 Fractional frequency offset (from arbitrary reference) versus pressure. (Absolute pressure known to only a factor of 2.)

FIG. 7 Drift of analog and digital comparator (demodulator) in time. Vertical scale calibrated in terms of equivalent frequency offset (error) introduced by comparator.

FIG. 8 Plot of phase spectral density $S_\phi(f)$ for locked and unlocked $\sim$ 0.5 GHz oscillator.

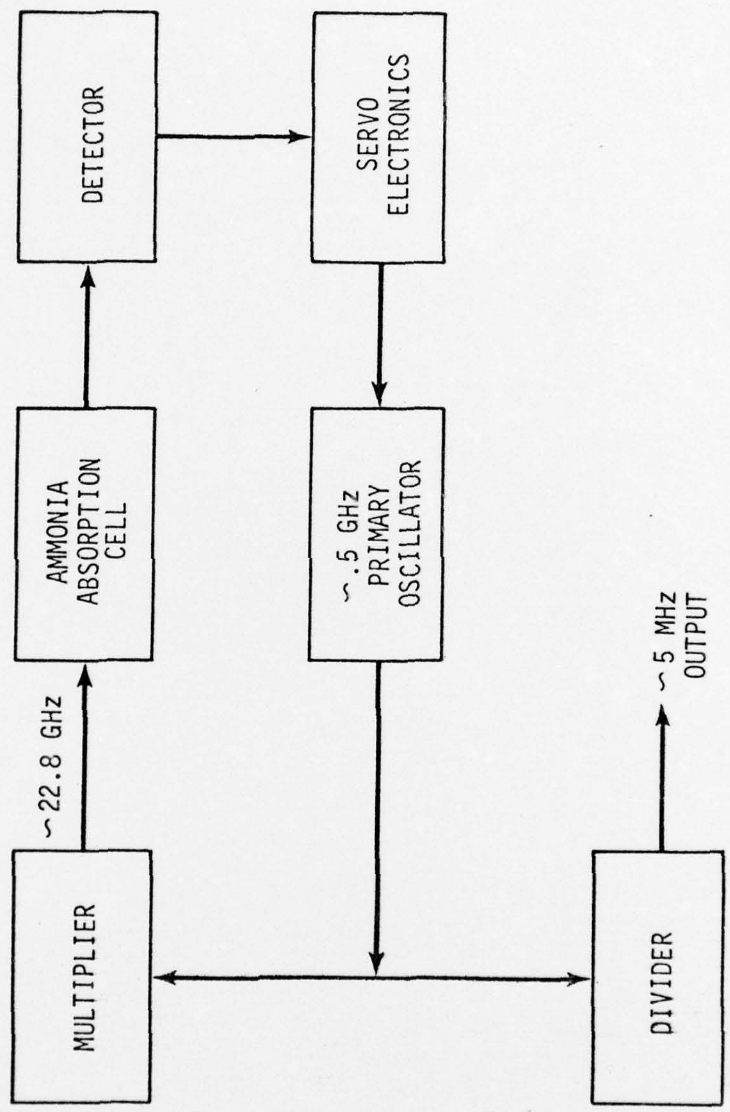
DETECTOR
SERVO
ELECTRONICS
AMMONIA
ABSORPTION
CELL
~ .5 GHz
PRIMARY
OSCILLATOR
~ 22.8 GHz
~ 5 MHz
OUTPUT
MULTIPLIER
DIVIDER

Fig. 1

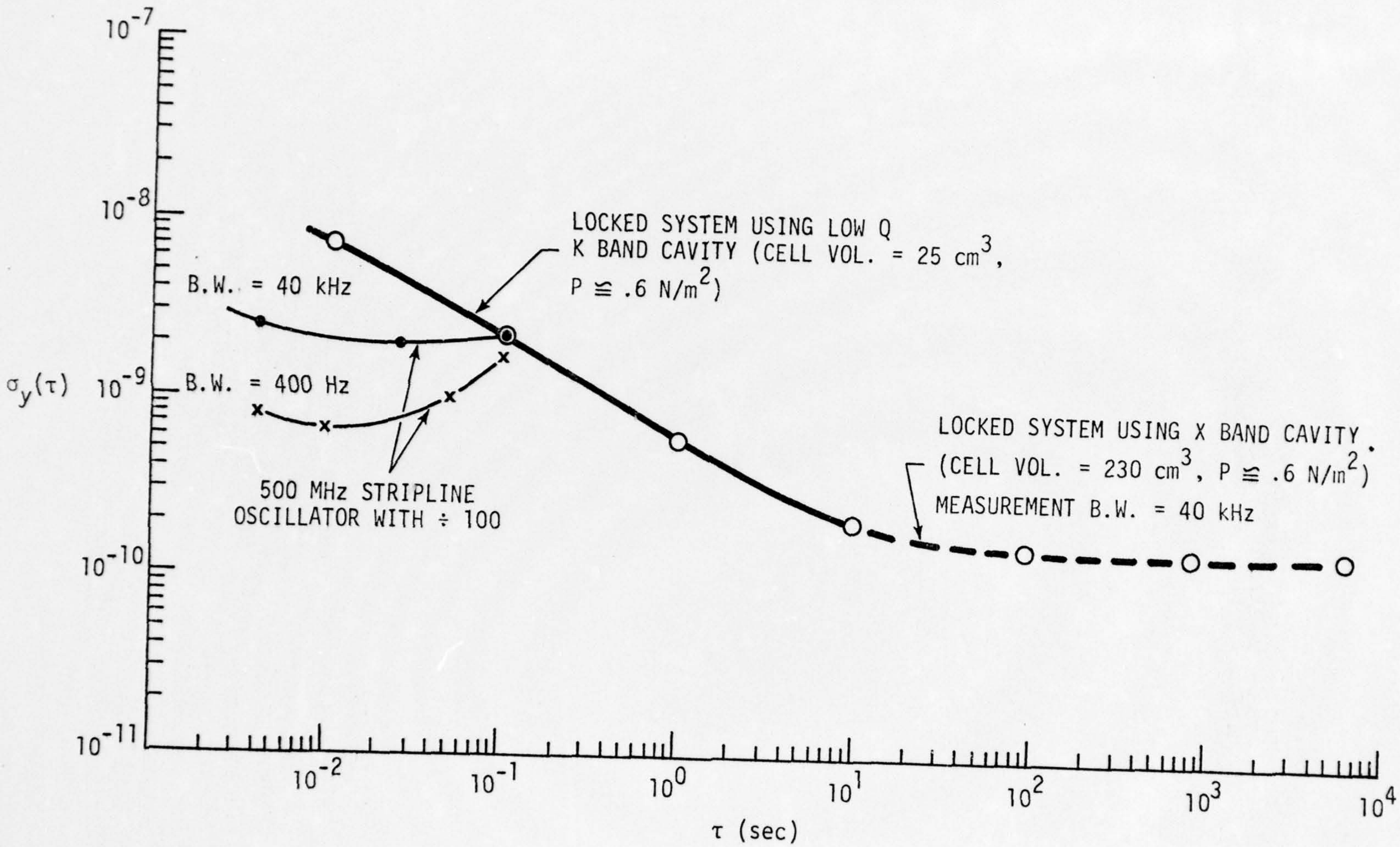

10^{-7}
10^{-8}
10^{-9}
10^{-10}
10^{-11}
$\sigma_y(\tau)$
B.W. = 40 kHz
B.W. = 400 Hz
LOCKED SYSTEM USING LOW Q
K BAND CAVITY (CELL VOL. = 25 cm^3,
P ≅ .6 N/m^2)
500 MHz STRIPLINE
OSCILLATOR WITH ÷ 100
LOCKED SYSTEM USING X BAND CAVITY.
(CELL VOL. = 230 cm^3, P ≅ .6 N/m^2)
MEASUREMENT B.W. = 40 kHz
10^{-2}
10^{-1}
10^{0}
10^{1}
10^{2}
10^{3}
10^{4}
τ (sec)

Fig. 2

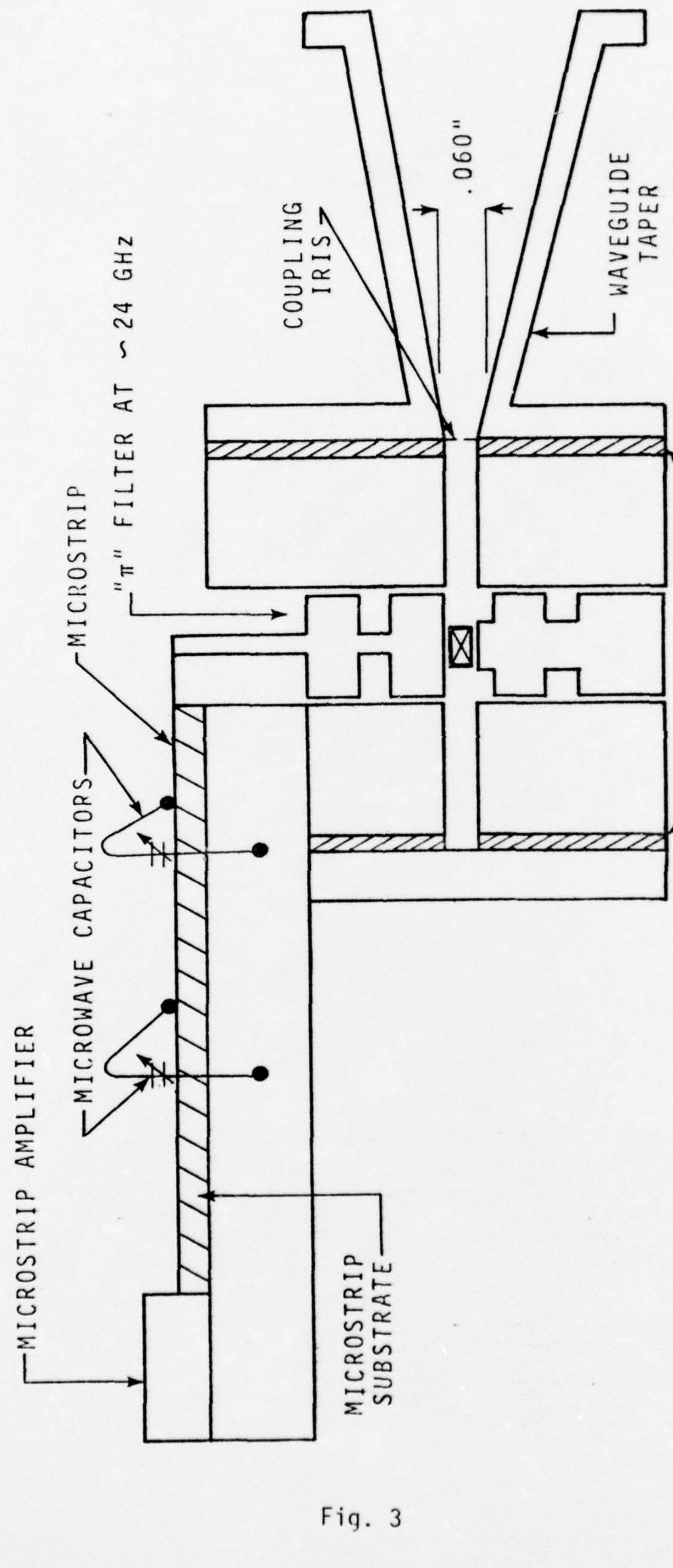

MICROSTRIP AMPLIFIER
MICROWAVE CAPACITORS
MICROSTRIP
"π" FILTER AT ~ 24 GHz
COUPLING IRIS
.060"
WAVEGUIDE TAPER
TUNING SHIMS
MICROSTRIP SUBSTRATE

Fig. 3

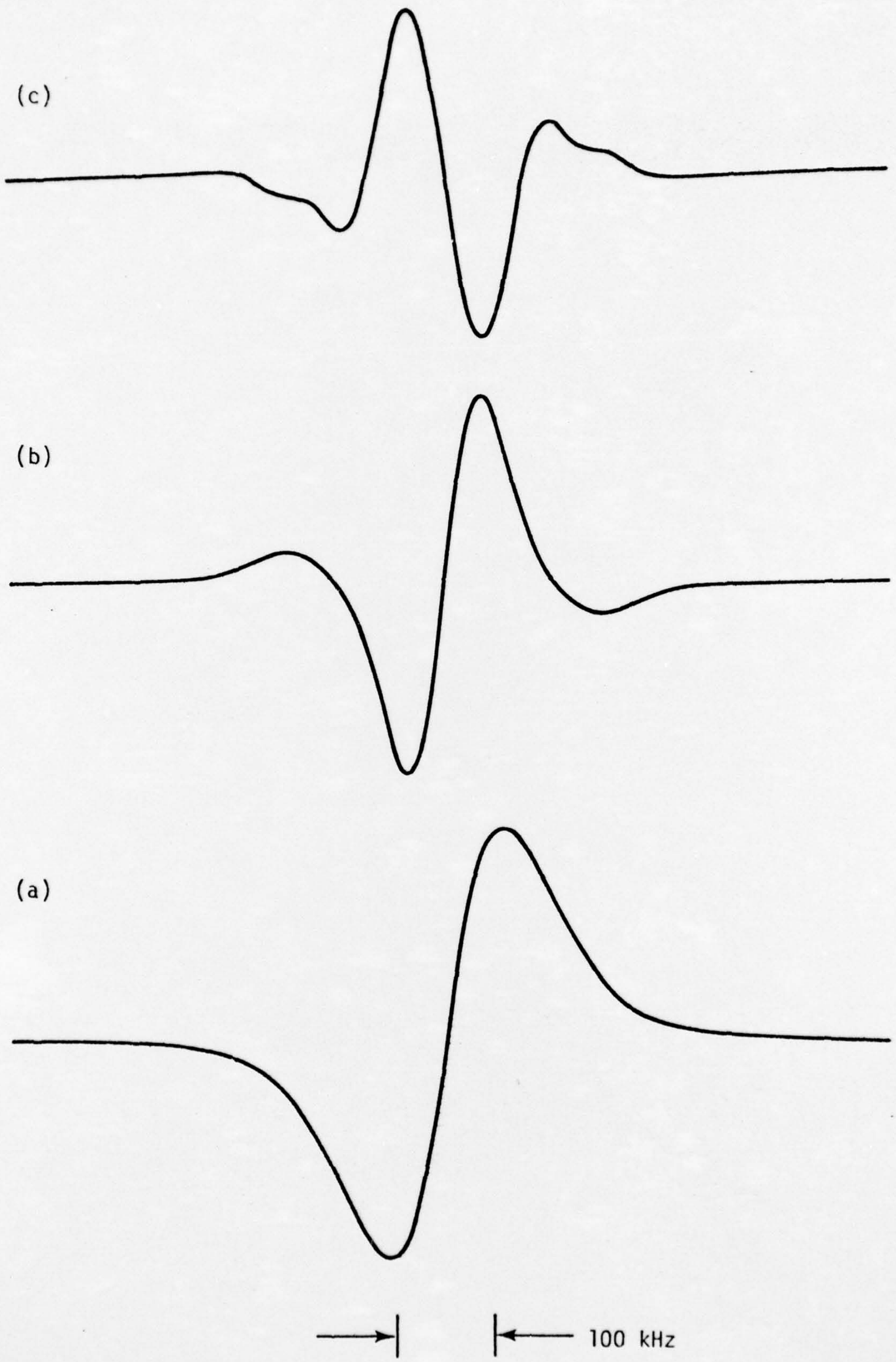

Fig. 4

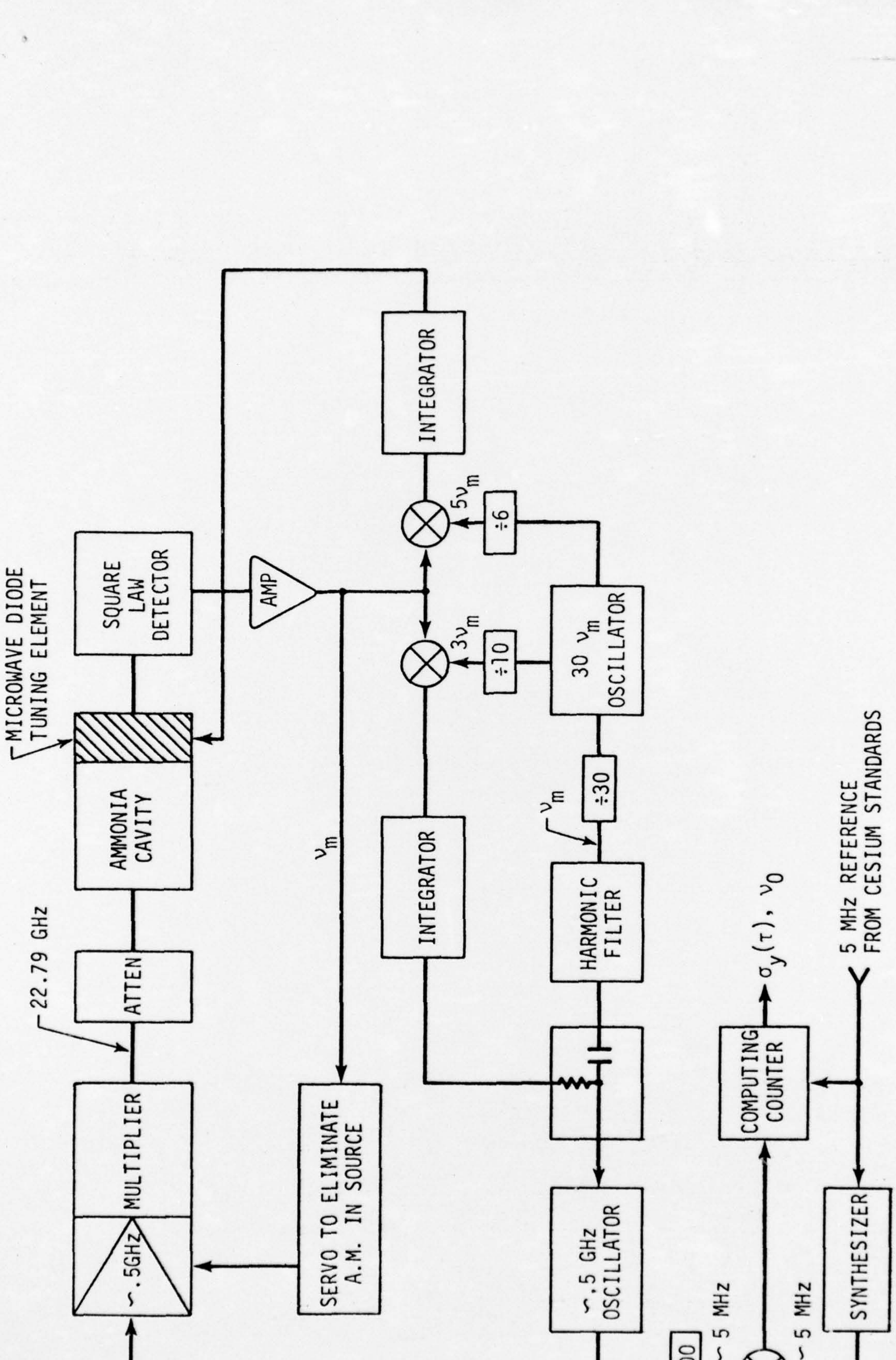

MICROWAVE DIODE TUNING ELEMENT
SQUARE LAW DETECTOR
AMP
INTEGRATOR
$5\nu_m$
÷6
$3\nu_m$
÷10
30 ν_m OSCILLATOR
÷30
ν_m
22.79 GHz
ATTEN
AMMONIA CAVITY
ν_m
INTEGRATOR
HARMONIC FILTER
MULTIPLIER
~.5GHz
SERVO TO ELIMINATE A.M. IN SOURCE
~.5 GHz OSCILLATOR
÷100
~5 MHz
~5 MHz
SYNTHESIZER
COMPUTING COUNTER
$\sigma_y(\tau)$, ν_0
5 MHz REFERENCE FROM CESIUM STANDARDS

Fig. 5

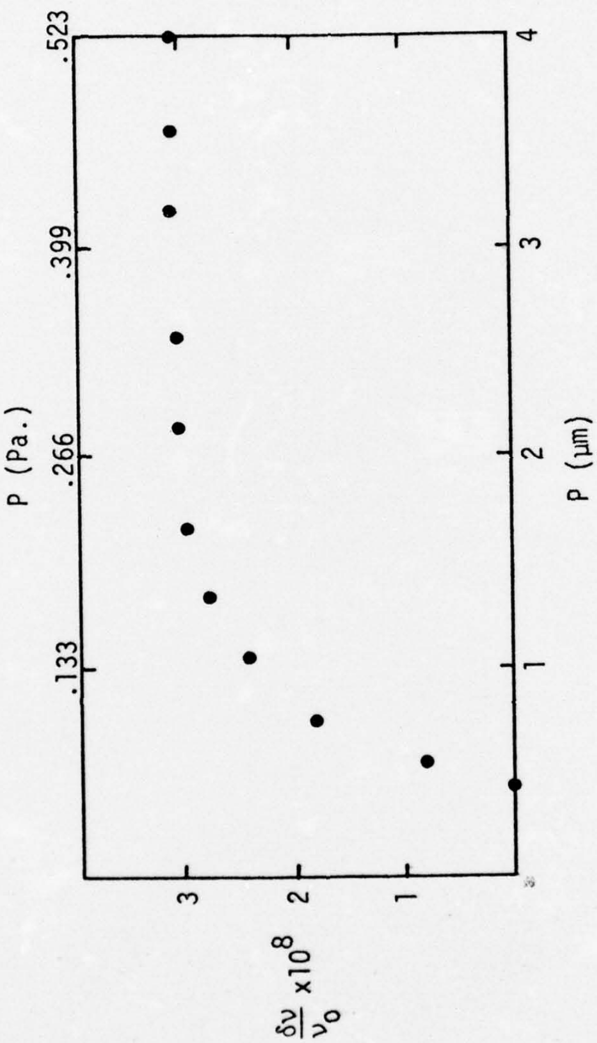

Fig. 6

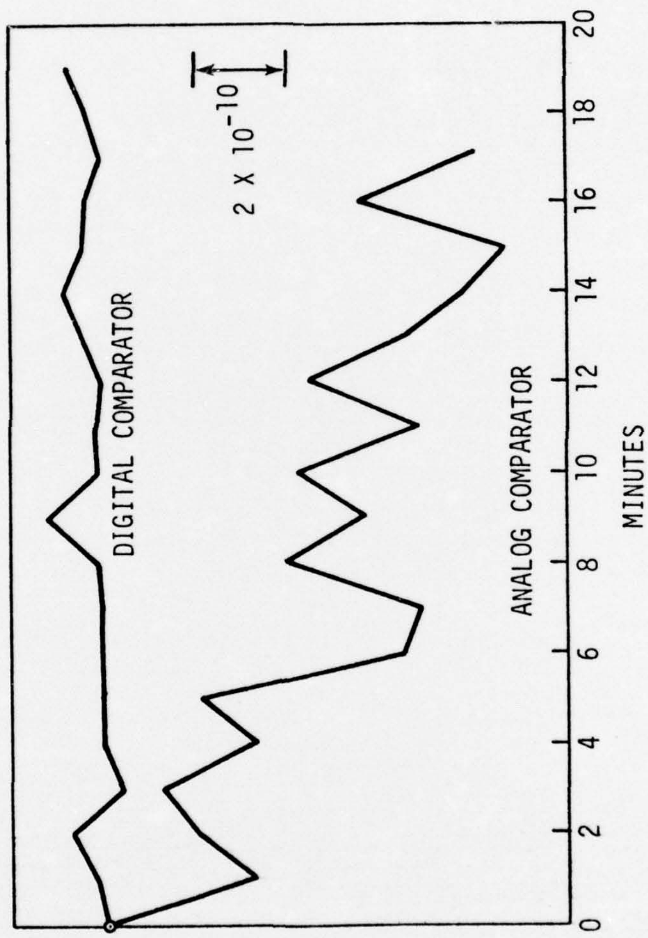
DIGITAL COMPARATOR
ANALOG COMPARATOR
2 X 10^-10
0
2
4
6
8
10
12
14
16
18
20
MINUTES

Fig. 7

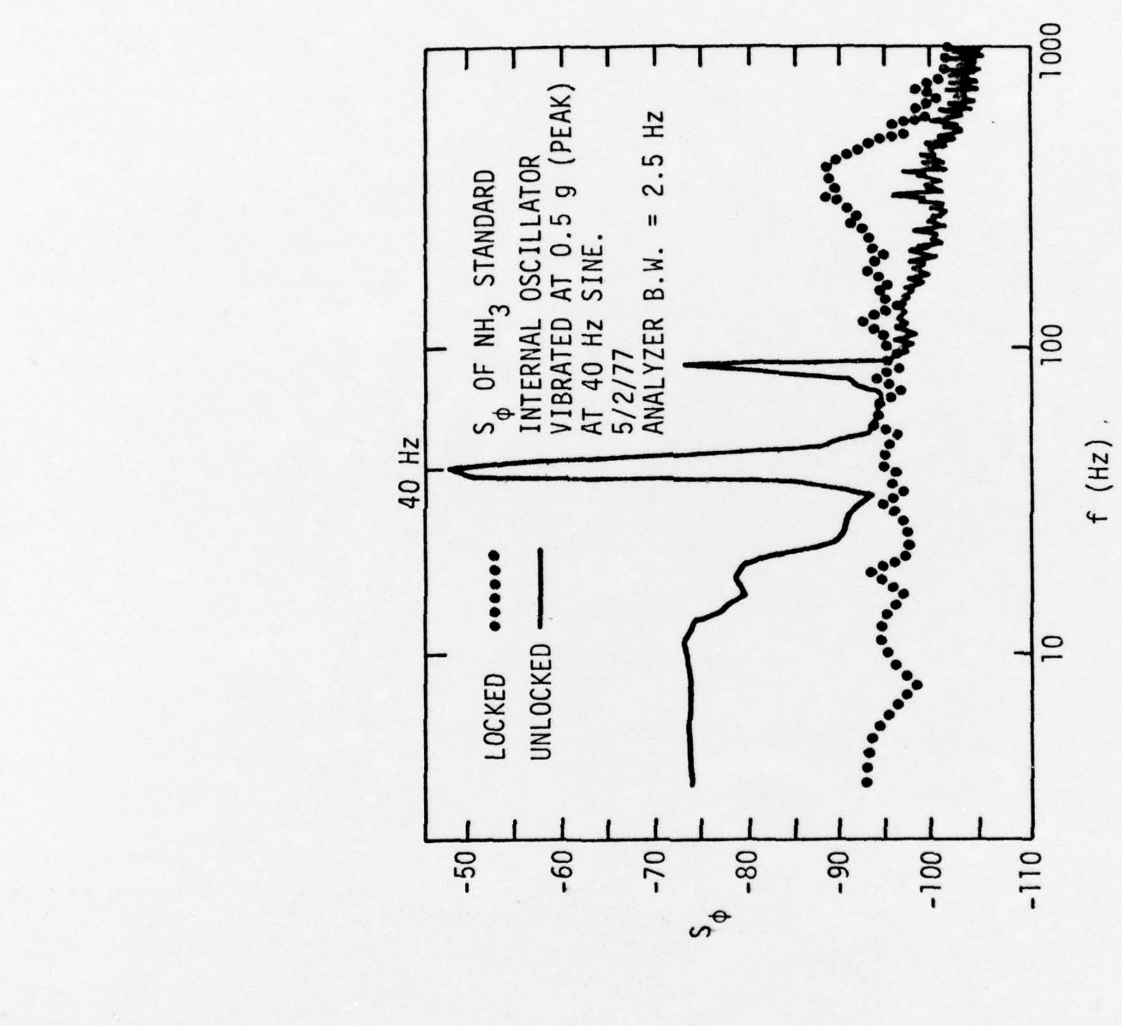
LOCKED
UNLOCKED
40 Hz
S_ϕ OF NH_3 STANDARD
INTERNAL OSCILLATOR
VIBRATED AT 0.5 g (PEAK)
AT 40 Hz SINE.
5/2/77
ANALYZER B.W. = 2.5 Hz
-50
-60
-70
-80
-90
-100
-110
S_ϕ
10
100
1000
f (Hz)

Fig .8